Title: Oxygen Vacancies as a Link between the Grain Growth and Grain Boundary Conductivity Anomalies in Titanium-rich Strontium Titanate

Authors: Alexander Tkach, Luís Amaral, Paula M. Vilarinho, Ana M.R. Senos

PII: S0955-2219(18)30029-3
DOI: https://doi.org/10.1016/j.jeurceramsoc.2018.01.014
Reference: JECS 11682

To appear in: *Journal of the European Ceramic Society*

Received date: 22-9-2017
Revised date: 10-1-2018
Accepted date: 11-1-2018

Please cite this article as: Tkach A, Amaral L, Vilarinho PM, Senos AMR, Oxygen Vacancies as a Link between the Grain Growth and Grain Boundary Conductivity Anomalies in Titanium-rich Strontium Titanate, *Journal of The European Ceramic Society* (2010), https://doi.org/10.1016/j.jeurceramsoc.2018.01.014

(revised version submitted to JECS, Ms. Ref. No.: JECS-D-17-01754R1, January 2018)

Oxygen Vacancies as a Link between the Grain Growth and Grain Boundary Conductivity Anomalies in Titanium-rich Strontium Titanate

Alexander Tkach,[a] *Luís Amaral,*[b] *Paula M. Vilarinho,*[a*] *Ana M. R. Senos*[a]

[a] CICECO – Aveiro Institute of Materials, Department of Materials and Ceramic Engineering, University of Aveiro, 3810-193 Aveiro, Portugal

[§] CeFEMA – Center of Physics and Engineering of Advanced Materials, Instituto Superior Técnico, University of Lisbon, 1049–001 Lisbon, Portugal

Corresponding Author

* Paula M. Vilarinho, paula.vilarinho@ua.pt

Titanium-rich (Sr/Ti=0.995) strontium titanate (ST) ceramics, air-sintered in a temperature range of 1400-1625 °C, were reported to possess anomalies in the grain growth and analogous anomalies in the grain boundary (GB) conductivity activation energy. However, these two interface-related phenomena, occurring at GBs, could not be associated with each other using a simple "brick-layer" model. In this work we revise the topic and advocate that the deviation from the model comes from the oxygen vacancies localized at GBs of the rapidly-cooled ST ceramics. To verify this, we annealed the ceramics in oxygen and performed their systematic and comparative analysis using impedance spectroscopy. A levelling-off in the GB conductivity activation energy, which increases for ≤1.2 eV, and a four-fold decrease in the GB permittivity are observed after annealing. Thus, we confirm a key role of oxygen vacancies in relation between the grain growth and GB conductivity anomalies of as-sintered Ti-rich ST ceramics.

KEYWORDS: strontium titanate, grain boundary specific area, vacancies, oxygen annealing, impedance spectroscopy, charge transport, conduction mechanism.

Introduction

There is a continued interest in strontium titanate-based materials, which have a great potential for a wide range of electronic applications. For instance, they can be used in tunable microwave devices due to the high electric-field dependence of the permittivity [1]. More recently, they were reported as promising thermoelectric materials [2]. Additionally, using strontium titanate ($SrTiO_3$, ST) as a model system, an understanding of the fundamental phenomena observed in the perovskite-type ABO_3 ionic oxides may be achieved, as was seen for investigations into the polar soft mode condensation [3,4] and the antiferrodistortive phase transition [5,6]. The electrical properties and crystal structure of these perovksite-type materials are well known to be closely related. They are also dependent on chemical stoichiometry and point defect chemistry, as oxygen vacancies, which can be controlled by either doping or sintering / annealing in different oxygen partial pressure conditions [7-10]. For example, the change in the concentration of the oxygen vacancies in $SrTiO_3$ by its reduction leads to the change of the electron concentration, and hence makes the system change from insulator to semiconductor, inducing as well a low-temperature superconducting phase transition [7]. Moreover, the antiferrodistortive phase transition was found to be suppressed by the increase in the concentration of the oxygen vacancies in ST-based systems [10].

The stoichiometry dependence of ST bulk properties has also been studied [8,11-13]. It was reported that ST with a Ti excess leads to coarse microstructures with enlarged grain size distributions [8,13], and to a Ti-rich second phase, appearing above 0.5 mol % excess [12]. On the other hand, Sr excess is fully accommodated in the perovskite lattice as a three-dimensional mosaic of single-layered rock-salt blocks, forming the so-called Ruddlesden-Popper structure [12], and usually results in finer microstructures with narrow grain size distributions [8,13]. The

different microstructure evolution was correlated with the defect chemistry induced by the nonstoichiometry [13]. Additionally, the TiO_2 excess was found to significantly raise the conductivity of ST, whereas only a slight increase was observed for SrO excess compositions [12].

Impedance spectroscopy (IS) was used to evaluate the bulk and grain boundary resistances (R_b and R_{gb}) of dense undoped ST ceramics as a function of their grain size [14,15]. The bulk conductivity did not depend significantly on the average grain size or grain size distributions, whereas the grain boundary (GB) conductivity varied with the average grain size, being however in incomplete agreement with the simple "brick-layer" model predictions [14]. The deviations from this model at moderate temperatures, more pronounced in the presence of reducing conditions, when the GB resistance decreases markedly with decreasing average grain size, were interpreted assuming enhanced conductivity along the GBs [15]. Furthermore, a grain growth anomaly, when the grain growth kinetics did not follow the classical Arrhenius-type temperature dependence, was recently reported in ST [16-18]. Two drops in the GB mobility were observed with the sintering temperature increasing from 1200 to 1600 °C independently of the Sr/Ti ratio [16]. Changes in the faceting behaviour of the GBs at high temperatures were suggested as the possible explanation for the anomalous grain growth behaviour [16,17]. More recently, some of the authors of the present work reported that 0.5 mol % Ti-rich ST ceramics possess three discontinuities in the grain growth, around 1500, 1550 and 1605 °C, at which the average grain size decreases despite the increasing sintering temperature [18]. Moreover, using IS and air atmosphere, similar discontinuities were observed in the activation energy of the GB conductivity due to a significant dispersion of the conductivity values measured around 500 °C [18]. However, the increased GB conductivity observed around 500 °C for the ceramics with the

smaller grain size, but not detected around 700 °C and not found for the ceramics with larger grain size over the entire measurement temperature range, could not be explained based on the simple "brick-layer" model. Indeed, this model assumes a continuous decrease of the GB conductivity with decreasing grain size due to the increasing number of insulating GBs, which the charge carriers should overcome [14].

In order to understand the origin of the discrepancy between the simple "brick-layer" model and observed results, and to find a relation between such interface-related phenomena as the grain growth and the GB conductivity, here we report a systematic IS study of the bulk and GB electrical evolution in 0.5 mol % Ti- rich ST ceramics sintered over a wide temperature range, and then annealed in oxygen.

Experimental Methods

Powders of $SrCO_3$ and TiO_2 (pro analysis (purity ≥99%), Merck) were mixed with a Sr/Ti ratio of 0.995 and ball milled in alcohol for 5 h, using a planetary mill, Teflon pots and zirconia balls. After calcination at 1100 °C for 2 h the ST powders were milled again under the same conditions. Then cylindrical pellets were uniaxially pressed at 50 MPa, isostatically pressed at 200 MPa and sintered in air for 2 h at twelve different temperatures between 1400 and 1625 °C. During sintering, the pellets were heated up and cooled down at the same rate of 15 °C min^{-1}. All the obtained ceramics reached a relative density >98%, as measured by the Archimedes method [18]. Annealing in oxygen was further performed with heating and cooling rate of 15 °C min^{-1} as well but the holding time was increased to 48 h, whereas the annealing temperatures were by 300±25 °C below the sintering temperature in order to not affect significantly the grain size. Particularly, ceramics sintered at 1575, 1590, 1600, 1610, and 1625 °C were annealed at 1300

°C, ceramics sintered at 1500, 1525, 1535, and 1550 °C were annealed at 1225 °C, and ceramics sintered at 1400, 1450, and 1475 °C were annealed at 1150 °C.

For the electrical characterization of Ti-rich ST ceramics, the opposite faces of the ceramic cylinders were polished to ensure parallel surfaces, and then silver paste electrodes were painted on them. Impedance spectroscopy (IS) measurements were carried out in air with a computer controlled precision LCR Meter (HP 4284A), under an applied ac field of 1 V in a frequency range 10^2-10^6 Hz and in a temperature range of 200-700 °C. Identically to the as-sintered case [18], the impedance data were collected on cooling with a rate of 4 °C min^{-1} after heating with the same rate to 700 °C for 5 min. Thus, we assure that any change observed in this work regarding the as-sintered ST ceramics is related to the effect of annealing in oxygen for 48 h at 1150-1300 °C, and not to the interaction with ambient atmosphere during the impedance measurements, which was relatively short and directed to the initial state of the ceramics. Then the data were normalized by being multiplied by the geometric factor A/h (A is the electrode area and h is the sample thickness) and analysed with the software ZView (Scribner Associates Inc.). To fit the impedance data, an equivalent circuit consisting of a series of three blocks of a resistor and a Constant Phase Element (CPE) in parallel, modelling bulk, GBs, and sample-electrode interface contributions, was used [18,19]. Fitting curve examples showing also a crossover from grain to grain boundary dominance at 450°C for the annealed ceramics in the frequency window of our impedance setup is shown in Fig. S1 (Supplementary Information).

Results and Discussion

Representative specific impedance complex planes of Ti-rich ST ceramics sintered between 1400 and 1625 °C and annealed in oxygen are plotted in Figure 1a and 1b for the

measurement temperatures of 300 and 600 °C, respectively. For both temperatures presented in Figure 1, well-resolved semicircles are observed. Their size varies with the sintering temperature by less than two-fold without any clear trend. On the other hand, as-sintered ceramics revealed a variation of around 5-6 times in the semicircle sizes, with a corresponding variation in the grain and GB resistances [18]. The semicircles are assigned to bulk and GB contributions, based on the magnitude of the capacitance values obtained by fitting the impedance data using the equivalent circuit approach [19]. At 300 °C (Figure 1a), the specific capacitance $C•h/A$ is in the order of 10^{-11} F cm^{-1}, indicating that the impedance spectra are mainly dominated by the bulk response. The GB contribution prevails at 600 °C (Figure 1b), where the capacitance is of the order of 10^{-8} F cm^{-1}.

Both bulk and GB capacitances of the ST ceramics annealed in oxygen are nearly temperature independent over the measurement range of this work. The representative capacitance values obtained at 300 °C for the bulk, and at 600 °C for the GB contribution, are presented in Figure 2 as functions of the sintering temperatures. The values obtained for as-sintered ceramics are presented in Figure 2 as well, for comparison. Similarly to the as-sintered ceramics [18], both bulk and GB capacitances of the oxygen-annealed ceramics are almost independent of the sintering temperature. Moreover, it can be seen that the bulk capacitance of ST ceramics annealed in oxygen is very close to that of as-sintered ceramics, the average for all the sintering temperatures being ~2×10^{-11} F cm^{-1}. In contrast, the average GB capacitance value is decreased by the oxygen annealing, from ~4×10^{-8} F cm^{-1} to ~1×10^{-8} F cm^{-1}.

Differently from the specific capacitance, the bulk and GB resistivities and, hence, conductivities of the oxygen-annealed ceramics (being thermally activated features) evidently depend on the measurement temperature. The Arrhenius plots ln(RA/h) vs 1000/T are shown in

Figure 3 (a-l) for their bulk and GB specific resistances. The values reported for as-sintered ceramics are also presented in Figure 3 for comparison. As seen from Figure 3, all the bulk conductivity values of the oxygen-annealed ceramics are consistent with the values of as-sintered ones [18]. Moreover, in the logarithmic scale they reveal also a linear dependence on the inverse temperature, with very similar slopes for all the sintering temperatures.

For the oxygen-annealed ceramics, the variation of the logarithm of the GB resistance values with the inverse temperature is also linear, as seen from Figure 3. Moreover, the line slopes are similar as well for all the sintering temperatures. This observation is in contrast to the as-sintered ceramics, where a marked variation of the slope with the sintering temperature, resembling the trend in variation of grain size, was observed. Correspondingly, the GB conductivity values of oxygen-annealed ceramics are not always close to that of as-sintered ones. Whereas at high temperatures (around 700°C) the values are rather similar, there is a significant difference in the moderate temperature range (around 500 °C), as marked by arrows in Figure 3 for the ceramics sintered at 1400, 1475, 1500, 1575, 1600 and 1610 °C. In addition, for these sintering temperatures, the GB resistance of as-sintered ceramics is comparable to, or even lower than, that of the bulk, whereas for all the oxygen-annealed ceramics, the GB resistance is higher than that of the bulk. For the rest of the sintering temperatures, the resistance values of as-sintered and annealed ceramics are quite similar over the whole measurement temperature range.

For a quantitative analysis and comparison, the values of the activation energy for both bulk and GB conductivities, $\sigma = 1/R$, were deduced from the line slopes in the Arrhenius plot, assuming an Arrhenius behaviour:

$$\sigma = \sigma_0 \exp^{\left(-\frac{E_a}{k_B T}\right)} \quad (1)$$

where σ_0 stands for the pre-exponential term, k_B for Bolzmann constant, T for absolute temperature and E_a for the activation energy of conductivity. Figure 4 shows the activation energy for the bulk and GB conductivities, obtained from the respective conductivity temperature dependences of the oxygen-annealed ceramics presented in Figure 3, as a function of sintering temperature. The values reported for as-sintered ceramics are shown in Figure 4 as well for comparison.

For the bulk conductivity, the activation energy E_b is around 0.9 eV, independent of the sintering temperature, which is in agreement with previously reported values for as-sintered ST ceramics [18]. For the GB conductivity, the activation energy E_{gb} varies from 1.64 to 1.90 eV, with a slight tendency to increase with increasing sintering temperature. In contrast, a much stronger variation of E_{gb} with the sintering temperature, from 0.46 to 1.76 eV, was observed for the as-sintered ceramics, resembling the trend of variation in grain size. Thus, the E_{gb} obtained in this work for the oxygen-annealed ceramics, being within 1.77±0.13 eV, corresponds to the highest E_{gb} value deduced for the as-sintered ceramics. At the same time, for the sintering temperatures of 1400, 1475, 1500, 1575, 1600 and 1610 °C, the E_{gb} values of the as-sintered and oxygen-annealed ceramics differ by as much as 0.67-1.24 eV. Such a difference is in agreement with the deviations in the GB conductivity, observed in the Arrhenius plots of corresponding ceramics at moderate temperatures (see Figure 3).

According to the results presented above, oxygen annealing of Ti-rich ST ceramics has three main effects on their high temperature electrical response:

i) the distribution of the impedance data for different sintering temperatures becomes about 3 times narrower than in as-sintered ceramics;

ii) the GB capacitance decreases by 4 times, whereas that of the bulk remains almost unchanged;

iii) the GBs of the smaller-grain-sized ceramics sintered at 1400, 1475, 1500, 1575, 1600 and 1610 °C become more resistive around 500 °C, while the bulk conductivity response stays the same. Correspondingly, the values of the E_{gb} increase, to equal the maximum values obtained for as-sintered ceramics, while the E_{gb} distribution becomes 5 times narrower.

Taking into account that the GB capacitance C_{gb} is determined by the following equation:

$$C_{gb} = \varepsilon_{gb}\, \varepsilon_0\, A_{gb} / d_{gb}, \quad (2)$$

where ε_0 is the vacuum permittivity, ε_{gb} is the permittivity, A_{gb} is the area and d_{gb} is the thickness of the GB, one could assume that its decrease by 4 times could be due to the corresponding increase in the GB thickness (since the grain size and, hence, A_{gb} is supposedly unaffected by annealing). Moreover, since the GB resistance R_{gb} is proportional to the GB thickness:

$$R_{gb} = \rho_{gb}\, d_{gb} / A_{gb}, \quad (3)$$

where ρ_{gb} is the resistivity of the GB, its increase at around 500 °C in the oxygen annealed ceramics sintered at 1400, 1475, 1500, 1575, 1600 and 1610 °C could also be explained, assuming that the GBs become thicker after annealing. Furthermore, variations in the GB

conductivity have been previously attributed to changes in the boundary thickness, for instance, in apatite-type electrolytes [20]. However, thanks to the wide set of the sintering and measurement temperatures used in this work, we have found that no significant variation of the GB resistance with oxygen annealing is observed around 500 °C for the other sintering temperatures, and around 700 °C for all the studied ceramics. Therefore, we can exclude the GB thickness as a key parameter for the modification of the electrical response in the Ti-rich ST ceramics. Instead, we should consider ε_{gb} and ρ_{gb} parameters and their relation with the possible alterations of the defect chemistry in STO.

As generally accepted, even undoped ST exhibits a specific concentration of acceptor impurities incorporated during processing or already present in the raw materials [21]. As result, oxygen vacancies and holes are formed. In addition, the incorporation of TiO_2-excess into the ST lattice in the current study requires the formation of strontium and oxygen vacancies [12,22] according to

$$TiO_2 \rightarrow V_{Sr}^{''} + Ti_{Ti} + 2O_O + V_O^{\bullet\bullet}. \quad (4)$$

Whereas strontium vacancies are known to be essentially immobile, oxygen vacancies are the main charge carriers within the grains at least under oxidative conditions and at the low-to-moderate temperatures of interest in this study [23,24]. Under oxidative conditions and moderate-to-high temperatures (>900 K), free holes are produced through the reaction between oxygen vacancies and atmospheric oxygen [23,25] according to

$$\frac{1}{2}O_2 + V_O^{\cdot\cdot} \Leftrightarrow O_O^{\times} + 2h^{\cdot}. \quad (5)$$

For the positive charge transport across the GBs the charge carriers should overcome a potential barrier of a space charge layer, since the oxygen-deficient GB has immobile positive charge that depletes the mobile positive charge carriers from the GB due to charge repulsion [26-28]. At the same time, a negative space charge of compensating electrons and other negative charges is accumulated on both sides of the GB [26-28]. As result, the activation energy of 1.77±0.13 eV obtained in this work for the GB conductivity of oxygen-annealed ceramics can be related to the double back-to-back Schottky barriers, formed by the space charge near the GBs, which the charge carriers contributing to the conductivity should overcome [27]. It should also be noted that after annealing in oxygen, E_{gb} becomes rather independent of the grain size in contrast to as-sintered ceramics, for which E_{gb} has been shown to follow the grain size variation [18]. Since the main effect of the annealing in oxygen is the suppression of the oxygen vacancy concentration, these vacancies have to be responsible for the link between E_{gb} and grain size in the as-sintered ceramics, although the corresponding mechanism is still unclear. Probably, contribution of conductivity along the grain boundaries [14,15] can occur in the case when $E_{gb} < E_b$ (see Figure 4) observed for some as-sintered ceramics with smaller grain size [18]. Moreover, for quantitative predictions within the space charge layer model, one should estimate the electron, hole and oxygen vacancy concentrations from the known value of TiO_2 excess, assuming its full incorporation into ST lattice and using Eq. (4). However, it is hard to find the hole concentration from uncontrolled acceptor impurities as well as the concentration of oxygen vacancies induced by processing conditions. Furthermore, in our further experiments on ceramics of this Ti-rich composition sintered at 1500 °C we have found that when heating/cooling rate is decreased from 15 to 5 °C/min, the GB activation energy increases from

0.91 to 1.48 eV despite of decrease in the average grain size from 17.5 to 7.5 μm [29]. Thus, besides the formation of oxygen vacancies it is important to quench them in order to be able to observe the correlation between the grain size and GB conductivity anomalies.

On the other hand, the activation energy for the bulk conductivity in undoped ST ceramics was reported to be of about 0.8 eV [30] whereas that for ST weakly doped with Ni was found to be of about 1 eV [27]. Thus, it looks reasonable to ascribe the activation energy of the bulk conductivity of around 0.9 eV obtained in the current work to the positive charge transport activation within the grains as well. Moreover, it is valid both for oxygen-annealed and as-sintered ceramics.

Concerning the permittivity, by definition, it is proportional to the localized charges able to polarize the material in response to an external electric field. Since the oxygen vacancies located at the GBs [28] represent a rather localized charge at low-to-moderate temperatures, the GB permittivity is dependent on the oxygen vacancy concentration. Therefore, when the concentration of such localized charges as oxygen vacancies is suppressed by annealing in oxygen, the GB dielectric permittivity, and hence the GB capacitance, decreases, as was observed in this work.

Conclusions

Impedance spectroscopy studies of oxidative annealing effects in titanium-rich ST ceramics provides new insights into the interface-related processes involved in the fabrication of electroceramics. Oxygen vacancy effects on the GB permittivity and resistivity are proposed to account for all the major features observed. Freshly sintered titanium-rich ST ceramics are oxygen deficient and have an anomalous grain size dependence with increasing sintering

temperature, revealing discontinuities at around 1500, 1550 and 1605 °C, at which temperatures the grain size decreases despite the increasing sintering temperature. Thus, for the smaller-grain-sized ceramics with larger GB specific area and, hence, high oxygen vacancy concentration, $E_{gb} < E_b$ probably due to the conduction mechanism along the GBs activated at low-to-moderate temperatures. During post-sintering oxygen annealing, grain surface oxidation occurs, leading to the the increase of the GB conductivity activation energy up to 1.77±0.13 eV. Moreover, the GB capacitance decreases from ~40 to ~10 nF cm^{-1} due to the suppression of the oxygen vacancy concentration and, hence, the GB permittivity during the annealing in oxygen.

Acknowledgements

This work was developed within the scope of the project CICECO-Aveiro Institute of Materials, POCI-01-0145-FEDER-007679 (FCT Ref. UID /CTM /50011/2013), financed by national funds through the FCT/MEC and when appropriate co-financed by FEDER under the PT2020 Partnership Agreement as well as within FCT independent researcher grant IF/00602/2013. L.A. acknowledges FCT for postdoctoral research grant SFRH/BPD/97453/2013. Thanks to Dr RC Pullar for assisting with the English language of this article.

References

1 A. K. Tagantsev, V. O. Sherman, K. F. Astafiev, J. Venkatesh and N. Setter, Ferroelectric Materials for Microwave Tunable Applications, J. Electroceram. 11 (2003) 5-66.

2 K. Koumoto, Y. F. Wang, R. Z. Zhang, A. Kosuga and R. Funahashi, Oxide Thermoelectric Materials: A Nanostructuring Approach, Annu. Rev. Mater. Res. 40 (2010) 363-394.

3 R. A. Cowley, Temperature Dependence of a Transverse Optic Mode in Strontium Titanate, Phys. Rev. Lett. 9 (1962) 159-161.

4 J. M. Worlock and P. A. Fleury, Electric Field Dependence of Optical-Phonon Frequencies, Phys. Rev. Lett. 19 (1967) 1176-1179.

5 H. Unoki and T. Sakudo, Electron Spin Resonance of Fe^{3+} in $SrTiO_3$ with Special Reference to the 110°K Phase Transition, J. Phys. Soc. Jpn. 23 (1967) 546-552.

6 P. A. Fleury, J. F. Scott and J. M. Worlock, Soft Phonon Modes and the 110°K Phase Transition in $SrTiO_3$, Phys. Rev. Lett. 21 (1968) 16-19.

7 J. E. Schooley, W. R. Hosler and M. L. Cohen, Superconductivity in Semiconducting $SrTiO_3$, Phys. Rev. Lett. 12 (1964) 474-475.

8 A. Tkach, P. M. Vilarinho, A. M. R. Senos and A. L. Kholkin, Effect of nonstoichiometry on the microstructure and dielectric properties of strontium titanate ceramics, J. Eur. Ceram. Soc. 25 (2005) 2769-2772.

9 A. Tkach, P. M. Vilarinho and A. L. Kholkin, Dependence of dielectric properties of manganese-doped strontium titanate ceramics on sintering atmosphere, Acta Mater. 54 (2006) 5385-5391.

10 A. Tkach, P. M. Vilarinho, A. L. Kholkin, I. M. Reaney, J. Pokorny and J. Petzelt, Mechanisms of the Effect of Dopants and $P(O_2)$ on the Improper Ferroelastic Phase Transition in $SrTiO_3$, Chem. Mater. 19 (2007) 6471-6477.

11 N. G. Eror, Defect Structure and Transport Properties of Titanates. In *Transport in Nonstoichiometric Compounds*, ed. G. Simkovich and V. S. Stubican. Plenum Press, NY, 1985, pp. 505-516 (and references therein).

12 Y. H. Han, M. P. Harmer, Y. H. Hu and D. M. Smyth, A^{++}/Ti Nonstoichiometry in Alkaline Earth Titanates, $ATiO_3$. In *Transport in Nonstoichiometric Compounds*, ed. G. Simkovich and V. S. Stubican. Plenum Press, NY, 1985, pp. 73-85 (and refrences therein).

13 L. Amaral, A. M. R. Senos and P. M. Vilarinho, Sintering kinetic studies in nonstoichiometric strontium titanate ceramics, Mater. Res. Bull. 44 (2009) 263-270.

14 J. C. C. Abrantes, J. A. Labrincha and J. R. Frade, Applicability of the brick layer model to describe the grain boundary properties of strontium titanate ceramics, J. Eur. Ceram. Soc. 20 (2000) 1603-1609.

15 J. C. C. Abrantes, J. A. Labrincha and J. R. Frade, Behavior of strontium titanate ceramics in reducing conditions suggesting enhanced conductivity along grain contacts, J. Eur. Ceram. Soc. 22 (2002) 1683-1691.

16 M. Baurer, D. Weygand, P. Gumbsch and M. J. Hoffmann, Grain growth anomaly in strontium titanate, Scr. Mater. 61 (2009) 584-587.

17 M. Baurer, H. Stormer, D. Gerthsen and M. J. Hoffmann, Linking Grain Boundaries and Grain Growth in Ceramics, Adv. Eng. Mater. 12 (2010) 1230-1234.

18 L. Amaral, M. Fernandes, I. M. Reaney, M. P. Harmer, A. M. R. Senos and P. M. Vilarinho, Grain Growth Anomaly and Dielectric Response in Ti-rich Strontium Titanate Ceramics J. Phys. Chem. C 117 (2013) 24787-24795.

19 J. T. S. Irvine, D. C. Sinclair and A. R. West, Electroceramics: Characterization by Impedance Spectroscopy, Adv. Mater. 2 (1990) 132-138.

20 D. Marrero-López, L. dos Santos-Gómez, L. León-Reina and J. Canales-Vázquez, Influence of the microstructure on the bulk and grain boundary conductivity in apatite-type electrolytes, J. Power Sources 245 (2014) 107-118.

21 R. A. De Souza, Oxygen Diffusion in $SrTiO_3$ and Related Perovskite Oxides, Adv. Funct. Mater. 25 (2015) 6326-6342.

22 S. Witek, D.M. Smyth and H. Pickup, Variability of the Sr/Ti Ratio in $SrTiO_3$, J. Am. Ceram. Soc. 67 (1984) 372-375.

23 P. C. McIntyre, Equilibrium Point Defect and Electronic Carrier Distributions near Interfaces in Acceptor-Doped Strontium Titanate, J. Am. Ceram. Soc. 83 (2000) 1129-1136.

24 R. Waser, Bulk Conductivity and Defect Chemistry of Acceptor-Doped Strontium Titanate in the Quenched State, J. Am. Ceram. Soc. 74 (1991) 1934-1940.

25 R. A. de Souza, The formation of equilibrium space-charge zones at grain boundaries in the perovskite oxide $SrTiO_3$, Phys. Chem. Chem. Phys. 11 (2009) 9939-9969.

26 Y. M. Chiang and T. Takagi, Grain-Boundary Chemistry of Barium-Titanate and Strontium-Titanate: I, High-Temperature Equilibrium Space-Charge, J. Am. Ceram. Soc. 73 (1990) 3278-3285.

27 R. Waser and R. Hagenbeck, Grain boundaries in dielectric and mixed-conducting ceramics Acta Mater. 48 (2000) 797-825.

28 R. F. Klie and N. D. Browning, Atomic scale characterization of oxygen vacancy segregation at $SrTiO_3$ grain boundaries, Appl. Phys. Lett. 77 (2000) 3737-3739.

29 L. Amaral, A. Tkach, P. M. Vilarinho, A. M. R. Senos, Nonstoichiometry and electrical response of strontium titanate ceramics, to be published.

30 P. Lupetin, G. Gregori and J. Maier, Mesoscopic Charge Carriers Chemistry in Nanocrystalline $SrTiO_3$, Angew. Chem. Int. Ed. 49 (2010) 10123-10126.

List of Figures

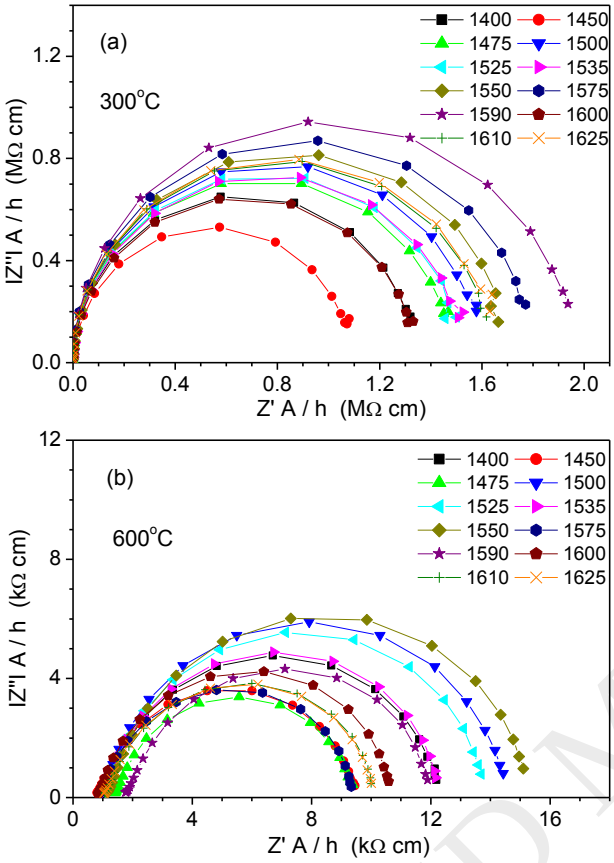

Fig. 1 Specific impedance complex plane plot at 300 (a) and 600 °C (b) for Ti-rich strontium titanate ceramics sintered between 1400 and 1625 °C and annealed in oxygen, revealing a moderate variation with the sintering temperature for both bulk and grain boundary responses, respectively.

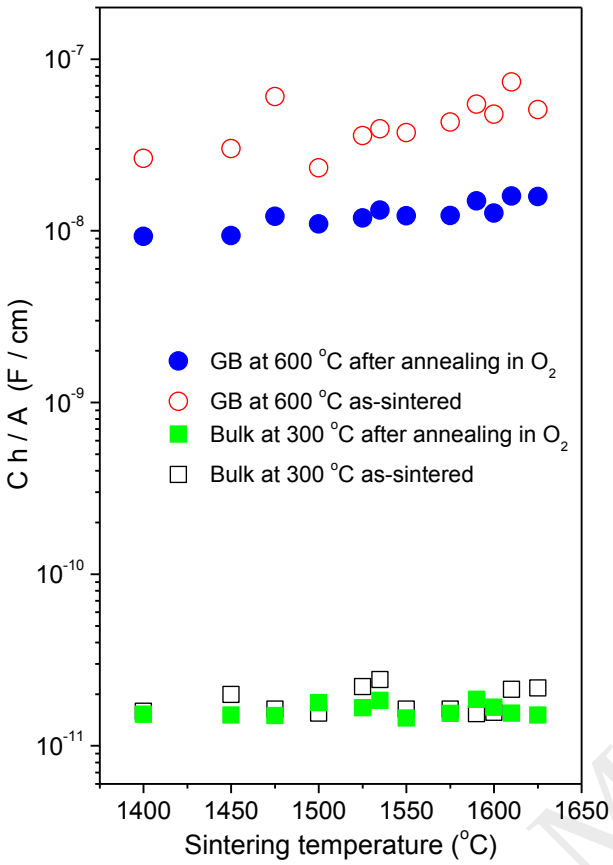

Fig. 2 Specific capacitance of bulk at 300 °C (squares) and grain boundaries at 600 °C (circles) of Ti-rich strontium titanate ceramics before (open symbols) and after (solid symbols) annealing in oxygen as a function of the sintering temperature. Bulk contribution keeps its value of ~$2x10^{-11}$ F/cm, whereas the grain boundary contribution decreases after annealing from ~$4x10^{-8}$ to ~$1x10^{-8}$ F/cm.

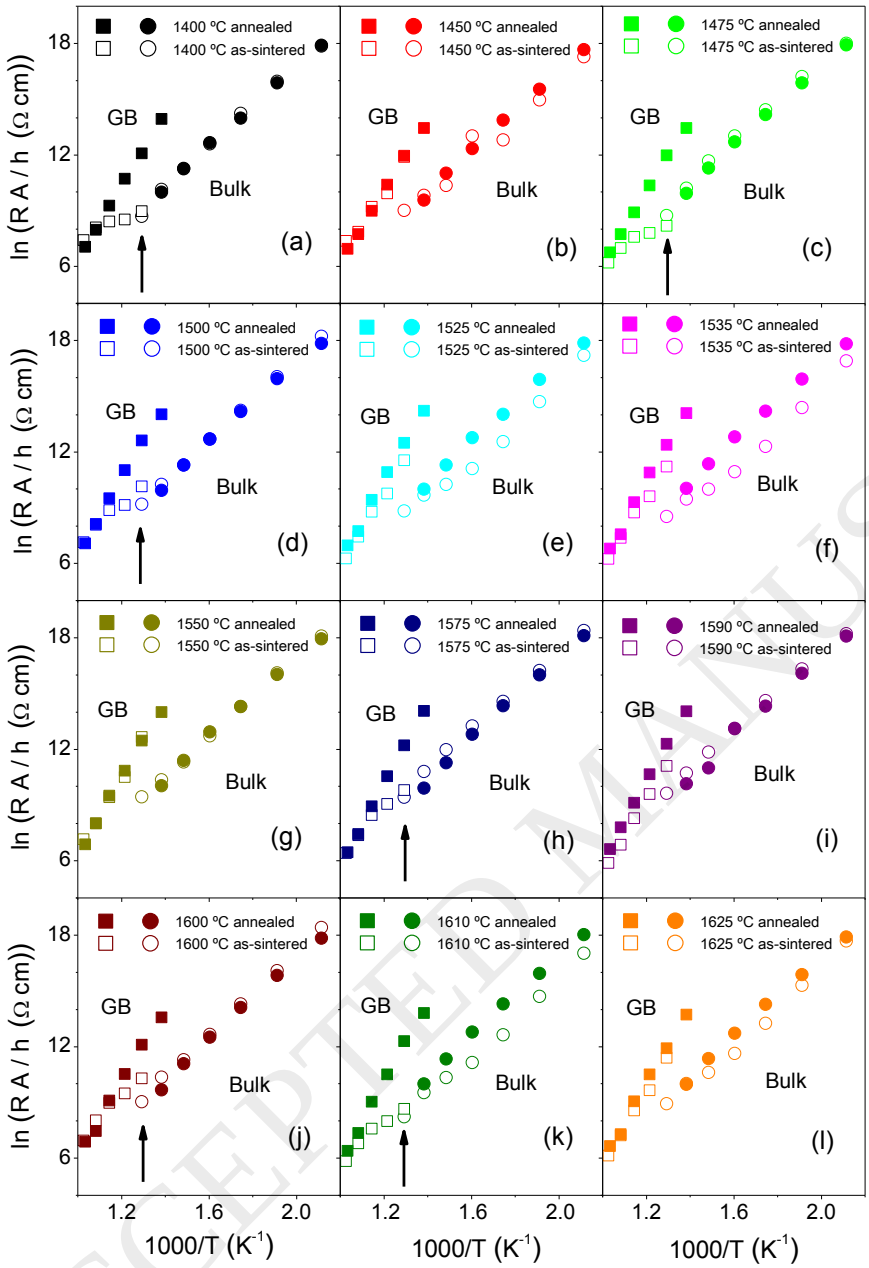

Fig. 3 Arrhenius plots for bulk (circles) and grain boundary (squares) specific resistance of Ti-rich strontium titanate ceramics sintered at 1400 (a), 1450 (b), 1475 (c), 1500 (d), 1525 (e), 1535 (f), 1550 (g), 1575 (h), 1590 (i), 1600 (j), 1610 (k), and 1625 °C (l) before (open symbols) and after (solid symbols) annealing in oxygen, revealing deviations in the grain boundary resistance for some samples as marked by arrows.

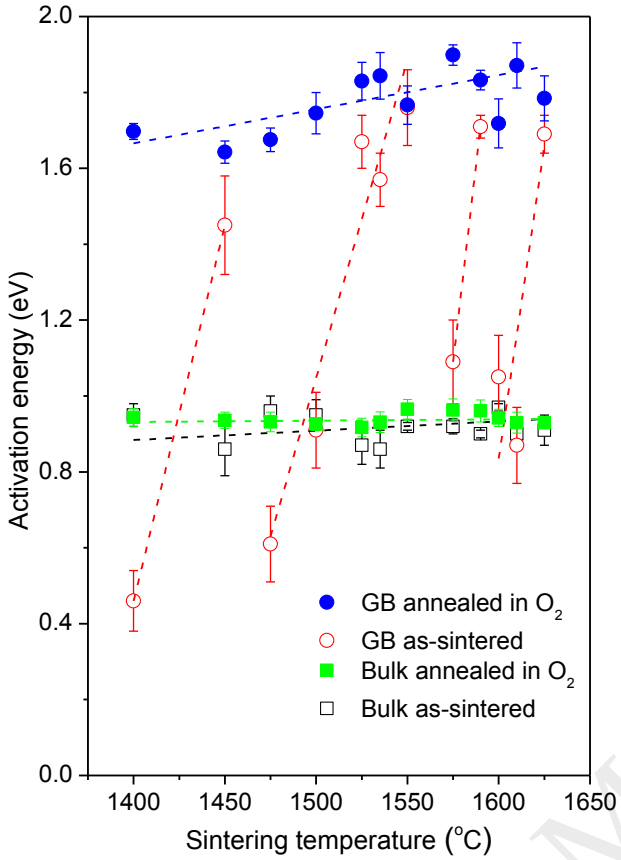

Fig. 4 Activation energy of bulk (squares) and grain boundary (circles) conductivity of Ti-rich strontium titanate ceramics before (open symbols) and after (solid symbols) annealing in oxygen as a function of the sintering temperature (data partly from Ref. 18), revealing a discontinuous variation for the grain boundary conductivity of as-prepared ceramics and a smooth variation for the grain boundary conductivity of oxygen-annealed ceramics.